Received: 11 October 2023 | Revised: 6 June 2024 | Accepted: 16 July 2024

DOI: 10.1002/eap.3048

ARTICLE

ECOLOGICAL APPLICATIONS
ECOLOGICAL SOCIETY OF AMERICA

Using spaceborne LiDAR to reveal drivers of animal demography

Brent R. Barry[1] | **Joseph D. Holbrook**[2] | **Jody C. Vogeler**[3] | **Lisa H. Elliott**[4] | **Matthew J. Weldy**[5] | **Damon B. Lesmeister**[6] | **Clinton Epps**[7] | **Todd Wilson**[6] | **Kerri T. Vierling**[4]

[1]Department of Environmental Science, University of Idaho, Moscow, Idaho, USA

[2]Department of Zoology and Physiology, Haub School of Environment and Natural Resources, University of Wyoming, Laramie, Wyoming, USA

[3]Natural Resources Ecology Laboratory, Colorado State University, Fort Collins, Colorado, USA

[4]Department of Fish and Wildlife Sciences, University of Idaho, Moscow, Idaho, USA

[5]Department of Forest Ecosystems and Society, Oregon State University, Corvallis, Oregon, USA

[6]Pacific Northwest Research Station, USDA Forest Service, Corvallis, Oregon, USA

[7]Department of Fisheries, Wildlife, and Conservation Sciences, Oregon State University, Corvallis, Oregon, USA

Correspondence
Brent R. Barry
Email: brbarry@uidaho.edu

Funding information
National Aeronautics and Space Administration, Grant/Award Number: 80NSSC21K0192; University of Idaho

Handling Editor: Sarah P. Saunders

Abstract

Remote sensing can provide continuous spatiotemporal information about vegetation to inform wildlife habitat estimates, but these methods are often limited in availability or lack adequate resolution to capture the three-dimensional vegetative details critical for understanding habitat. The Global Ecosystem Dynamics Investigation (GEDI) is a spaceborne light detection and ranging system (LiDAR) that has revolutionized the availability of high-quality three-dimensional vegetation measurements of the Earth's temperate and tropical forests. To date, wildlife-related applications of GEDI data or GEDI-fusion products have been limited to estimate species habitat use, distribution, and diversity. Here, our goal was to expand the use of GEDI-based applications to wildlife demography by evaluating if GEDI data fusions could aid in characterizing demographic parameters of wildlife. We leveraged a recently published dataset of GEDI-fusion forest structures and capture–mark–recapture data to estimate the density and survival of two small mammal species, Humboldt's flying squirrel (*Glaucomys oregonensis*) and Townsend's chipmunk (*Neotamias townsendii*), from three studies in western Oregon spanning 2014–2021. We used capture histories in Huggins robust design models to estimate apparent annual survival and density as a derived parameter. We found strong support that both flying squirrel and chipmunk density were associated with GEDI-fusion forest structures of foliage height diversity and plant area volume density in the 5–10 m strata for flying squirrels and proportionately higher plant area volume density in the 0–20 m strata for chipmunks, as well as other spatiotemporal factors such as elevation. We found weak support that apparent annual survival was associated with GEDI-fusion forest structures for flying squirrels but not for chipmunks. We demonstrate further utility of these methods by creating spatially explicit density maps of both species that could aid management and conservation policies. Our work represents a novel application of GEDI data to evaluate wildlife demography and produce continuous spatially explicit density predictions for these species. We conclude that aspects of small mammal demography can be explained by forest structure as characterized via GEDI data fusions.

KEYWORDS
density, foliage height diversity, forest structure, full waveform, GEDI, *Glaucomys oregonensis*, LiDAR, *Neotamias townsendii*, plant area volume density, survival

INTRODUCTION

Ecologists have long recognized that vegetation structure plays a critical role in wildlife habitat and biodiversity (e.g., MacArthur & MacArthur, 1961). The configuration and composition of vegetation have been shown to strongly influence aspects of habitat such as forage quality, diversity, and availability (Cook et al., 2016; Johnson et al., 2001), predation avoidance (Moriarty et al., 2016), foraging efficiency (Andruskiw et al., 2008), thermoregulation (Alston et al., 2020), intraguild interactions (Finke & Denno, 2002), and reproductive success (Kosterman et al., 2018). Embedded within these relationships is the spatial scale at which animals interact with vegetation and how these species–habitat associations change with scale (McGarigal et al., 2016) ranging from the microsite (e.g., localized canopy cover or cavity characteristics) to the landscape (e.g., patch size and orientation; Johnson, 1980; Turner et al., 2001). Thus, comprehensive assessments of how different species relate to horizontal and vertical vegetative structures across a range of spatial scales and ecosystems are critical to inform data-driven conservation and management strategies.

Remote sensing can provide spatiotemporal information about vegetation that aids in defining habitat, but data describing vertical structure are often difficult to obtain despite studies that suggest it is an important or essential habitat feature for some species (Fuller et al., 2004; Jaime-González et al., 2017). The Global Ecosystem Dynamics Investigation (GEDI) aims to revolutionize the availability of high-quality three-dimensional vegetation measurements of the Earth's temperate and tropical forests across unprecedented, near-global scales (Dubayah et al., 2020). GEDI is a spaceborne light detection and ranging system (LiDAR) that offers widely spaced, moderate-scale full waveform LiDAR footprints (25 m). In this regard, GEDI provides great promise for measuring habitat components but lacks spatially continuous metrics that better represent the biological processes influential to habitat (Gaillard et al., 2010) or that can be more readily incorporated into conservation and management planning. A recently published dataset used GEDI footprints as a vertical and horizontal sampling source to develop continuous data-fusion products characterizing GEDI metrics at 30-m resolution (hereafter GEDI-fusion products; Vogeler et al., 2023) and prior efforts have demonstrated value in using these GEDI-fusion products to understand species–habitat relationships (Elliott et al., 2024; Smith et al., 2022; Vogeler et al., 2023).

A primary objective of the GEDI mission is to determine how forest structure affects habitat quality and biodiversity (Dubayah et al., 2020). To date, applications of GEDI to address this objective have been focused primarily on modeling species distributions (Burns et al., 2020; Elliott et al., 2024; Killion et al., 2023; Smith et al., 2022) which relate species occurrence (i.e., presence or presence–absence) to environmental conditions to estimate realized distributions (Elith & Leathwick, 2009; McLoughlin et al., 2010). Spatial variation in the occurrence of species is thought to reflect habitat quality through the selection of habitat that maximizes fitness benefits (Fretwell & Lucas, 1969). However, occurrence provides a less robust measure to distinguish between habitats of high and low quality as compared to variation in population demographics (Johnson, 2007). Demographic parameters (e.g., survival, recruitment, density) are the highest standard in understanding habitat quality because they differentiate between where populations thrive or merely persist (Pulliam, 2000). Despite these benefits, there have been no attempts to link direct GEDI measurements or GEDI-fusion products to wildlife demographic parameters to identify more meaningful habitat quality metrics.

Vertical structure has been shown to be crucial to birds (e.g., MacArthur & MacArthur, 1961) and other arboreal species (e.g., Froidevaux et al., 2016; Gubert et al., 2023; Linnell et al., 2017) but these attributes also significantly impact terrestrial small-bodied mammals (Jaime-González et al., 2017; Sullivan et al., 2000). Small mammals relate to structural habitat variables such as the age, structure, and heterogeneity of forest stands, understory vegetation, and microsite features like coarse woody debris or snags (Carey, 1995; Ecke et al., 2002; Fuller et al., 2004; Schooler & Zald, 2019; Sullivan et al., 2000). Traditional airborne LiDAR can effectively characterize some of these structural features and be used to link forest structure to small mammal habitat use, diversity, and abundance (Hatten, 2014; Jaime-González et al., 2017; Linnell et al., 2017; Nelson et al., 2005; Schooler & Zald, 2019). Thus, small mammals are ideal subjects to evaluate GEDI-fusion products on wildlife demography because these populations are sensitive to forest structure and can be monitored with capture–mark–recapture techniques

to obtain demographic parameters. If small mammal demography is associated with forest structures measured by GEDI data, then managers can leverage GEDI's broad coverage to apply species–habitat associations estimated from small-scale studies to whole management units or ecosystems by projecting these species–habitat associations to unsampled landscapes. Further, spatially explicit maps that link demographic parameters to GEDI-derived forest structures can be used in predictive frameworks to guide management decisions by showing how changes in vegetation affect demography with unprecedented resolution.

In the Pacific Northwest, USA, the effects of forest structure on small mammal populations have been an important area of research since the early 1990s to understand the impacts of forest management practices and inform conservation planning for imperiled species. Two of the most well-studied species are Humboldt's flying squirrel (*Glaucomys oregonensis*) and Townsend's chipmunks (*Neotamias townsendii*; hereafter GLOR and NETO) because they are ecologically important (Carey et al., 1992; Forsman et al., 2004), relatively abundant, and habitat structure has been suggested to drive population density patterns (Carey, 1995; Wilson, 2010). GLOR was recently distinguished from *Glaucomys sabrinus* (Arbogast et al., 2017), and high densities are linked with characteristics typical of, but not limited to, old forest characteristics such as multi-layering (i.e., variance in stem density) and high canopy cover (Holloway & Smith, 2011; Rosenberg & Anthony, 1992; Weldy, Epps, et al., 2019; Wilson, 2010). Predation (i.e., survival) mediated through forest structure has been hypothesized to limit GLOR populations (Wilson, 2010; Wilson & Forsman, 2013). NETO habitat preferences are flexible but still associated with forest structures like large diameter trees, canopy cover, elevation, and well-developed understories, particularly berry-producing shrubs (Carey, 1995; Weldy, Epps, et al., 2019). High NETO densities are found in old-growth forests (Hayes et al., 1995) and regenerating early seral forests that retain structure (Sultaire et al., 2021). Lower NETO densities have been found in second-growth forests (Rosenberg & Anthony, 1993) and clearcuts without retained structure (Sultaire et al., 2021).

This study investigates the associations among GEDI-fusion products depicting horizontal and vertical forest structure and the density and survival of two small mammal species, Humboldt's flying squirrel (*G. oregonensis*) and Townsend's chipmunks (*N. townsendii*). Here our objectives were as follows: (1) estimate apparent annual survival and its association with forest structure, (2) estimate site-level annual density of each species, (3) optimize the environmental variables to their most predictive spatial scale with respect to density, (4) assess the importance of these scaled variables to density associations, and (5) extrapolate our density predictions to unsampled localities. We hypothesized that GEDI-fusion products would explain spatial variation in apparent annual survival and density estimation for GLOR, as this species is strongly influenced by forest structures. We hypothesized that NETO would be more weakly associated with forest structure compared to GLOR because they are considered more habitat generalists but are still associated with some forest structural components.

METHODS

Study areas

We used previously collected data from three previous study areas in western Oregon, USA: the H. J. Andrews Experimental Forest (hereafter, HJA), the Siuslaw National Forest (hereafter, SIU), and the Umpqua National Forest (hereafter, UMP; Figure 1). Conditions varied at each site according to their study design and intent. The HJA is a late-successional research forest on the western slope of the Cascade Mountains. Sites located in the HJA were stratified by canopy openness and elevation from 683 to 1244 m. Forest conditions were dominated by large (>81 cm dbh) Douglas-fir (*Pseudotsuga menziesii*), western hemlock (*Tsuga heterophylla*), and Pacific silver fir (*Abies amabilis*; Cissel et al., 1999; Schulze & Lienkaemper, 2015). SIU and UMP sites were stratified by young—managed and old-growth—unmanaged stands distributed across the Siuslaw National Forest in the Coast Range and within the Tiller district of the Umpqua National Forest in the Cascades, respectively (Figure 1). These sites were dominated by Douglas-fir and western hemlock, but elevations differed between 264–596 m on SIU sites and 735–1321 m on UMP sites. The weather for all study areas was typically hot and dry May–September and cool and wet October–April. Average annual precipitation varies from 2068–2386 mm on HJA, to 2064–3223 mm on SIU sites, and 1025–1319 mm on UMP sites (PRISM Climate Group, Oregon State University, https://prism.oregonstate.edu, data created 4 February 2014, accessed 9 January 2024). Precipitation occurs primarily during winter with rain at low elevations (<1000 m) and snow at high elevations (>1000 m).

Environmental data

We considered 14 a priori covariates (Table 1) that reflect animal–environment relationships previously described

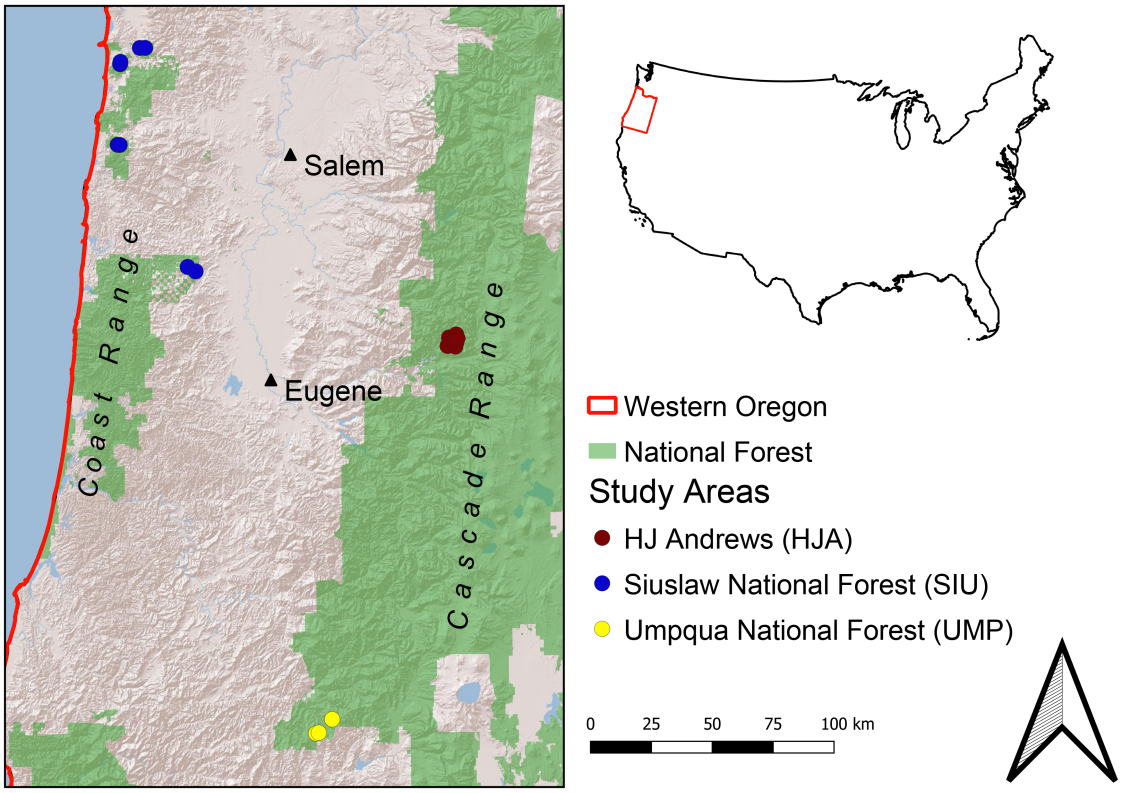

FIGURE 1 Study area and trapping grid locations from western Oregon, USA. There were nine trapping grids at the H. J. Andrews Experimental Forest (HJA), eight on the Siuslaw National Forest (SIU), and three on the Umpqua National Forest (UMP).

in the literature and additional hypotheses about the species. For topographic features, we used a digital elevation model developed from the Shuttle Radar Topography Mission (SRTM; Farr et al., 2007) downloaded from Google Earth Engine (Gorelick et al., 2017). From this, we were able to obtain elevation and compute slope, aspect, and topographic position index (mTPI; Guisan et al., 1999) using Google Earth Engine. Other abiotic factors considered were annual precipitation of each trapping year (PPT), annual mean minimum temperature (TMin), and mean maximum temperature (TMax) to index climate variability. PPT, TMin, and TMax were obtained for each trapping year from the PRISM climate group (PRISM Climate Group, Oregon State University, https://prism.oregonstate.edu, data created 4 February 2014, accessed 9 September 2022).

We used GEDI-fusion products of forest structure that were originally published in Vogeler et al. (2023); full details on the generation, validations, and additional descriptions of each covariate can be found therein. Briefly, GEDI-fusion products were modeled using random forest machine learning frameworks leveraging a variety of continuous remote sensing data predictors (i.e., Landsat, Sentinel-1, topographic features, climate, and forest disturbance) to produce continuous maps of forest structure at 30-m resolutions. We included seven of these GEDI-fusion covariates in our analyses because they characterize features we hypothesized would be important to GLOR, NETO, or both (Figure 2; Table 1). Canopy cover (COVER) is a representation of vegetative cover and an estimate of the amount of light that penetrates the canopy to the forest floor. Foliage height diversity (FHD) characterizes how vegetation is distributed vertically throughout the canopy and can be thought of as a measure of vertical heterogeneity or multilayering. The plant area volume density metrics describe the proportion of the vegetation within each pixel that is either; (1) above 40 m (PAVD_40) which is used as an old-growth indicator, (2) above or below 20 m (PAVD_20) which can be used to describe dense vegetation's orientation in the canopy, and (3) between 5 and 10 m (PAVD_5_10) which is the lowest strata available and used as our best representation of a shrub/understory layer. The relative height indices describe the maximum height (RH98) and midpoint (in meters) where there are comparable amounts of vegetation above and below (RH50; Figure 2).

Animal data

We used capture–mark–recapture live-trapping data that was collected as part of previous studies that followed

TABLE 1 Density covariates, sources, and optimized spatial scales for *Glaucomys oregonensis* (GLOR) and *Neotamias townsendii* (NETO).

Covariate	Optimized scale in ha		Source	Description
	GLOR	NETO		
Elev	136.89 (1170 m^2)	10.89 (330 m^2)	SRTM	Elevation in m
mTPI	10.89 (330 m^2)	10.89 (330 m^2)	SRTM	Topographic position index—distinguishes ridge from valley by subtracting local elevation from 1.2 km neighborhood mean elevation
Slope	136.89 (1170 m^2)	136.89 (1170 m^2)	SRTM	Slope
Aspect	15.21 (390 m^2)	75.69 (870 m^2)	SRTM	Aspect
PPT	4 km^2	4 km^2	PRISM	Annual precipitation
TMIN	4 km^2	4 km^2	PRISM	Annual mean minimum temperature
TMAX	4 km^2	4 km^2	PRISM	Annual mean maximum temperature
Cover	20.25 (450 m^2)	10.89 (330 m^2)	GEDI	Percent canopy cover—the amount of light able to penetrate the canopy to the forest floor
FHD	32.49 (570 m^2)	15.21 (390 m^2)	GEDI	Foliage height diversity—Shannon–Weiner index of height diversity within a pixel, multilayered canopies
PAVD_5_10	15.21 (390 m^2)	136.89 (1170 m^2)	GEDI	Plant area volume density within 5–10 m, our best approximation for shrubs
PAVD_20	56.25 (750 m^2)	136.89 (1170 m^2)	GEDI	Plant area volume density above 20 m
PAVD_40	136.89 (1170 m^2)	10.89 (330 m^2)	GEDI	Plant area volume density above 40 m, indicator of old-growth conditions
RH50	56.25 (750 m^2)	15.21 (390 m^2)	GEDI	Relative height at the 50th percentile of the return
RH98	20.25 (450 m^2)	15.21 (390 m^2)	GEDI	Relative height at the 98th percentile of the return

Note: Covariates were obtained from the Shuttle Radar Topography Mission (SRTM), PRISM Climate Group (PRISM), or the Global Ecosystem Dynamics Investigation (GEDI).

similar methodologies (see *Trapping design* below) but differed in some ways (Weldy, Epps, et al., 2019; Weldy, Wilson, et al., 2019; Weldy et al., 2020; and others). Sites at the HJA were designed to understand how small mammal dynamics varied within late-successional forests, while sites at SIU and UMP were intended to understand how small mammal dynamics varied between old forests (i.e., unmanaged) and young—managed stands. Thus, HJA sites are clustered within a late-successional reserve and stratified by factors important to old-growth characteristics (i.e., openness and elevation), while SIU and UMP sites are widely dispersed and stratified by management history. Collectively, these sites represent samples from a range of forest conditions typical of temperate Pacific Northwest forests. We leverage data from these study areas collected between 2014 and 2021 to estimate the density and survival of GLOR and NETO. The HJA contained nine sites that were trapped from 2014 to 2018, three of which were also trapped in 2019 and 2021. The SIU and UMP were trapped from 2014 to 2016 and consisted of eight sites and three sites. In total, these data represent 84 site-years for density and survival estimates.

Trapping design

Each study area used similar designs; for full design and details see (Carey, 1991; Weldy et al., 2020; Weldy, Wilson, et al., 2019). Briefly, at each site, 64 trap stations were arranged in an 8×8 array (7.84 ha) with slope corrected 40 m distance between traps. At each trap station, two Tomahawk Model 201 live traps (Tomahawk Live Trap, WI, USA) were placed within 5 m of the trap station center ($n = 128$ traps per site). Sites were trapped for three consecutive weeks between September and early

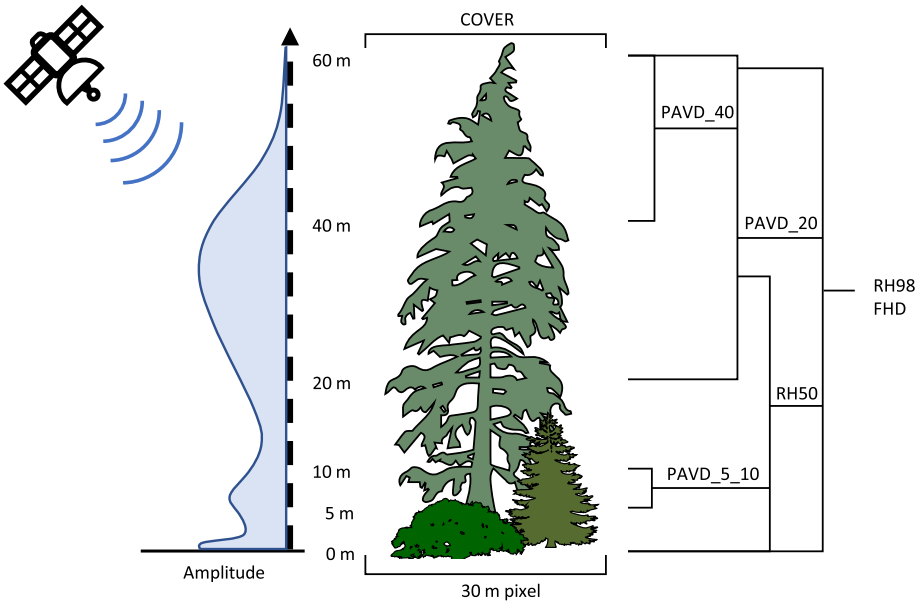

FIGURE 2 Conceptual figure describing how vegetation is measured by the Global Ecosystem Dynamics Investigation (GEDI) and how the GEDI-fusion variables relate to vegetation structure. COVER, canopy cover; FHD, foliage height diversity; PAVD_5_10, plant area volume density between 5 and 10 m; PAVD_20, plant area volume density above or below 20 m; PAVD_40 = plant area volume density above 40 m; RH50, relative height of 50% of vegetation; RH98, relative height of 98% of vegetation. See Table 1 for additional covariate descriptions. Image credits: Satellite by Brent R. Barry; *Tsuga heterophyla* by Ian Burt (original) and T. Michael Keesey (vectorization) available under a CC BY 3.0 license (https://creativecommons.org/licenses/by/3.0/) with no modifications made to the image for this work except for color; *Pseudotsuga* is free of known restrictions; *Ficus sycomorus* is in the public domain.

December where each week was comprised of four consecutive trap nights (i.e., a total of 12 trapping nights per site per year). At the HJA sites, NETO was trapped for only two consecutive weeks due to high recapture rates (i.e., 8 nights) and GLOR was trapped for 3 weeks in 2014–2016 and 2 weeks in 2017–2021. Traps were baited, checked, and reset once per day. Individuals were tagged with unique ear tags and reproductive condition, species, sex, and body weight (in grams) were recorded. Trapping protocols were consistent with the American Society of Mammalogists guidelines (Sikes & Animal Care and Use Committee of the American Society of Mammalogists, 2016) and conducted under the appropriate permits (USDA Forest Service Starkey IACUC number 92-F-0004 and Oregon State University's ACUP number 4191, 2011–2013; number 4590, 2014–2016).

Capture analysis

We used individual capture histories and Huggins robust design models (Kendall et al., 1995, 1997) to estimate apparent annual survival (φ), recapture probability (c), initial capture probability (p), immigration (γ'), emigration (γ''), and density (N) as a derived parameter. The robust design leverages both primary occasions (in years) and secondary sampling occasions (trapping session) to estimate parameters. Capture and recapture probabilities are estimated from within secondary occasions using the Huggins component (Huggins, 1989, 1991). Apparent annual survival (henceforth, survival), temporary immigration, and emigration are estimated between primary occasions using the Cormack–Jolly–Seber component (Cormack, 1964; Jolly, 1965; Seber, 1965). We used the Huggins robust design model to ensure that our density estimates were consistent with previous studies (e.g., Weldy, Epps, et al., 2019), to account for the potential effects of emigration on survival (Weldy et al., 2022), and to provide inference on whether survival was associated with forest structure.

To estimate density and determine whether survival was associated with forest structure we considered several model specifications. We fit a series of model structures for parameters γ', γ'', p, and c, using covariates representing the most likely sources of variation (Weldy, Wilson, et al., 2019; Appendix S1: Table S1) and considered these to be nuisance parameters because they are important to produce accurate estimates but we did not wish to draw inference from them. We included model specifications that allowed for trapping behavioral effects and different immigration/emigration movement patterns (no movement, random

movement, Markovian movement, and movement that varied by trapping grid or study area). We modeled each parameter sequentially (starting with γ' and γ'', then p, c, and finally φ) and used the most supported parameterizations while holding unmodeled parameters at a near-global model (Appendix S1: Table S1). We selected the best-supported model for each parameter using Akaike information criterion, corrected for small sample sizes (AIC_c; Burnham & Anderson, 2002). A null intercept-only model was included to evaluate model performance relative to models parameterized by covariates. We considered the model with the lowest AIC_c and models within two AIC_c units as competitive (Burnham & Anderson, 2002). Finally, we tested φ's association with forest structure using univariate or bivariate GEDI-fusion variables (Table 1), a GEDI-fusion variable and a source of variation (e.g., FHD and year), or two sources of variation (e.g., study area and year). GEDI variables represented the mean value calculated from a focal window of 330 × 330 m (10.89 ha; see *Environmental data* for more details) with the trapping grid centroid at the center. This focal window was chosen to reflect conditions of the trapping grid, 7.84 ha, and a buffer to account for tagged individuals that used space outside of the grid. We limited models to no more than two covariates for each parameter due to small sample sizes and to avoid overfitting. All models were implemented in RMark (Laake, 2013) using program R (R Core Team, 2023).

Scale optimization

In our second phase of modeling, we optimized the spatial scale for each covariate following McGarigal et al. (2016). We considered model covariates at multiple spatial scales using analytical tests to determine the strongest correlated response, where each spatial scale was the mean covariate value of an $n \times n$ window of pixels centered on the geometric centroid of each trapping grid. Our finest resolution was an 11 × 11 window of 30 m pixels (10.89 ha) and we increased each spatial scale by odd values (e.g., 11 × 11, 13 × 13, 15 × 15, etc.), ensuring the grid centroid was centered, to a maximum of 39 × 39 window size (136.89 ha), resulting in 15 spatial scales. We assumed our finest scale would represent the local characteristics of each trapping grid, while our broadest scale would reflect conditions influencing the larger population dynamics.

We optimized the spatial scale for each covariate from univariate generalized linear mixed models with negative binomial error distributions and a log link. The negative binomial was chosen after dispersion values of models fit with Poisson error distributions indicated overdispersion greater than 1.10. We specified our model as follows:

$$\log(y) = a + \beta X^{ij} + \beta\text{Study} + \gamma\text{Site} + \gamma\text{YearStudy}, \quad (1)$$

where our response variable y was the density estimated for each year a trapping grid was sampled and X^{ij} represented the mean values of covariate i at scale j. Study is a fixed effect of HJA, SIU, and UMP. Each trapping grid, Site, was treated as a normally distributed random effect (Gillies et al., 2006; Shirk et al., 2014) and we allowed unmodeled annual temporal variation to vary by study area using a normally distributed random effect, YearStudy. We determined the scale with the most predictive power by the lowest AIC score (Shirk et al., 2014; Tweedy et al., 2019; Wasserman et al., 2010). The spatial scale of PPT, TMin, and TMax was fixed at 4 km^2 from PRISM, and as such we did not conduct scale optimization for these variables.

We used the LandTrendR (Landsat Detection of Trends in Disturbance and Recovery) algorithm (Kennedy et al., 2010) on Google Earth Engine (Kennedy et al., 2018) to ensure accurate representations of site conditions at each spatial scale by screening for disturbance when animal data and environmental data were not temporally aligned. We verified that no major disturbances had occurred within our study areas and at spatial scales considered despite several large wildfires and timber harvests that occurred nearby.

Density and habitat

We used the density estimates, N, from our most supported robust design parameterizations as our response variable. We developed a set of 16 multivariate generalized linear mixed models with negative binomial error distributions to account for overdispersion (Bolker et al., 2009; Zuur et al., 2009). Each model represented a hypothesis we considered reasonable for predicting density from remotely sensed variables. These a priori hypotheses used only covariates at their optimized scale and were developed consistent with the literature. For example, some models used only GEDI-fusion products or only abiotic variables, while others used combinations of GEDI and abiotic variables to best represent plausible biological hypotheses regarding the drivers of density (Appendix S1: Table S2). All models included three or less environmental covariates to avoid overfitting. Model specifications were similar to Equation (1) but we modified βX^{ij} to be vector of covariates i at their optimized scale, j. To avoid problems associated with multicollinearity between selected scales and covariates in our models, we

computed Pearson's correlation coefficients. Covariates with a Pearson's correlation value of $|r| \geq 0.7$ were not included in the same model. All covariates were standardized to have a mean of 0 and SD of 1. We assess the importance of each covariate by magnitude and direction of its effect size and CI. We used bootstrapping ($n = 5000$) to estimate the variance of fixed and random effects using the merTools package (Knowles & Frederick, 2019) included in Appendix S1.

We again evaluated candidate models using AIC_c and considered competitive models within $\Delta AIC_c \leq 2$ (Burnham & Anderson, 2002). We were unable to average models due to high collinearity between covariates in different models (Cade, 2015). To ensure that our results were robust to uncertainty in our density estimation, we reran the top models with annual site densities at their upper and lower 95% CI's, and have provided those materials in the Appendix S1. We assessed model fit by checking each model for overdispersion by dividing the sum of the squared Pearson residuals by the residual df. Values close to 1 suggest data without overdispersion (Bolker et al., 2009; Zuur et al., 2009). In addition, we calculated both the conditional R^2 and marginal R^2 to assess the model fit and compare the variance explained by random effects versus fixed effects (Nakagawa & Schielzeth, 2013). We used the lme4 package (Bates et al., 2014) in program R for all models.

To extrapolate predictions about unsampled areas, we applied the fixed coefficients from the top model for each species to the GEDI-fusion and topographic rasters to calculate a spatially explicit index of density for each species. We considered this an index because these values do not account for temporal variation and thus are not predictions of population size at a given time. Rather, these predictions use the spatial drivers identified from our models to describe general patterns of density. We capped the effect of elevation at 1800 m, the approximate tree line for this region.

RESULTS

Our dataset included 1276 individual GLOR across all years and study areas. At the nine HJA sites, 976 individuals were captured from 2014 to 2021. At the eight SIU sites, 201 individuals were captured from 2014 to 2016, and on the three UMP sites, 99 individuals were captured from 2014 to 2016. From the same period and sites, 4088 individual NETOs were captured, including 2882 from the HJA, 820 from the SIU, and 386 from UMP sites. Trap nights totaled 64,512 for GLOR and 51,456 for NETO.

The final specifications for nuisance parameters (γ', γ'', p, and c) of both species are included in Appendix S1: Tables S3–S6, respectively. GLOR daily recapture probabilities varied widely from 0.07 (95% CI [0.05–0.10]) to 0.39 (95% CI [0.35–0.42]) but generally decreased within each trapping session and tended to peak on day 5 (Appendix S1: Figure S1). The probability of initial capture for GLOR ranged from 0.03 (95% CI [0.01–0.05]) to 0.28 (95% CI [0.25–0.30]) and tended to be highest on HJA sites, lowest on SIU sites, and intermediate on UMP sites (Appendix S1: Figure S2). For NETO, daily recapture probabilities ranged from 0.24 (95% CI [0.21–0.28]) to 0.78 (95% CI [0.75–0.81]) and were generally higher on HJA sites than UMP or SIU sites despite the reduced trapping period (8 and 12 days, respectively; Appendix S1: Figure S1). Capture probabilities followed a similar pattern to recapture rates and tended to be higher on HJA sites than UMP or SIU sites, ranging from 0.04 (95% CI [0.01–0.24]) to 0.43 (95% CI [0.37–0.50]). Temporary immigration (γ') and emigration (γ'') varied highly between sites for NETO (Appendix S1: Table S7).

The top-ranking GLOR survival model contained year and study area (Appendix S1: Table S8). Survival estimates from this model varied from 0.26 (95% CI [0.18–0.36]) in 2018 at HJA to 0.54 (95% CI [0.34–0.73]) in 2015 at SIU (Figure 3; Appendix S1: Table S9). All competitive GLOR survival models contained either year alone ($\Delta AIC_c = 0.19$) or year and a GED-fusion covariate (year + COVER: $\Delta AIC_c = 0.18$, year + FHD: $\Delta AIC_c = 1.48$, year + PAVD_5_10: $\Delta AIC_c = 1.62$, year + RH50: $\Delta AIC_c = 1.98$; Appendix S1: Table S8). From these competitive models, the effect of forest structure was generally consistent with our hypotheses suggesting dense vegetation increased survival; however, the effect sizes were small and CI's overlapped zero (Figure 3). Survival for NETO was generally lower than GLOR but similarly was best explained by year and study area (Appendix S1: Table S8). Estimates from this model ranged from 0.19 (95% CI [0.12–0.28]) in 2015 at UMP to 0.47 (95% CI [0.32–0.64] in 2014 at SIU; Figure 3; Appendix S1: Table S9). NETO survival models that contained a GEDI-fusion covariate were not competitive ($\Delta AIC_c = 4.7$; Appendix S1: Table S8) but were the best-ranking models following study area and year.

We report the mean (SD), min, and max annual site density from each study area, while the full site- and year-specific estimates can be found in Appendix S1: Figure S3. From the top-ranking GLOR survival model, annual densities ranged from 1.43 to 9.59/ha and a mean of 4.0/ha (1.58) at HJA. Annual site densities averaged 3.54/ha (2.52) and ranged from 0 to 8.63/ha on SIU sites. UMP sites averaged 3.45/ha (1.49) with a minimum of 0.99/ha and a maximum of 6.16/ha. NETO densities

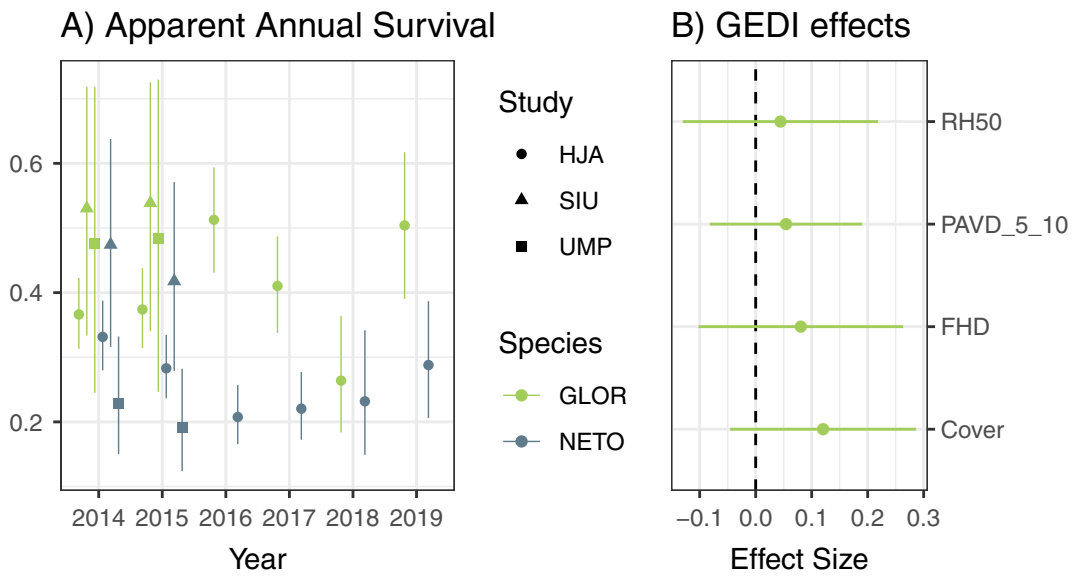

FIGURE 3 Survival estimates and effects of forest structure with 95% CI's. (A) shows survival estimates from each study area (HJA, H. J. Andrews Experimental Forest; SIU, Siuslaw National Forest; UMP, Umpqua National Forest) per year for each species (GLOR, *Glaucomys oregonensis*; NETO, *Neotamias townsendii*). (B) depicts the Global Ecosystem Dynamics Investigation (GEDI) covariates (Cover, canopy cover; FHD, foliage height diversity; RH50, relative height of 50% of vegetation; PAVD_5_10, plant area volume density between 5 and 10 m) from competitive survival models. There were no competitive Neotamias townsendii models that contained GEDI covariates. Note that there were no competitive survival models for *Neotamias townsendii* that contained GEDI covariates.

varied widely between sites and study area, from a minimum of 2.74/ha to a maximum of 18.8/ha on HJA sites averaging 9.44/ha (3.89), 0.69/ha to 15.7/ha on SIU sites averaging 5.75/ha (4.84), and 3.91/ha to 13.5/ha on UMP sites averaging 7.86/ha (6.51).

Following our scale optimization procedure, we identified the most correlated spatial scale for each covariate (Table 1). Generally, the effect size, statistical significance, and AIC_c values trended either up or down as the spatial extent grew larger (Appendix S1: Figure S4). The effect of some variables switched from positive to negative at small to large scales, suggesting scale-mediated effects.

Here we report only competitive density models but include all results in the supporting information (Appendix S1: Table S10). Variables are presented as variable (spatial scale, $\beta \pm$ SE, p value). For GLOR we found the best-supported density model incorporated topographic position index (mTPI, 10.89 ha, $\beta = -0.15 \pm 0.09$, $p = 0.10$), foliage height diversity (FHD, 26.01 ha, $\beta = 0.44 \pm 0.11$, $p < 0.00$), and plant area volume density between 5 and 10 m (PAVD_5_10, 15.21 ha, $\beta = 0.26 \pm 0.10$, $p < 0.01$; Figure 4). The influence of random effects (Site and YearStudy) was relatively small (var = 0.11, SD = 0.33, and var = 0.017, SD = 0.13, respectively) except for Sites in the SIU (Appendix S1: Figure S5). One model was competitive ($\Delta AIC_c = 1.86$) and contained similar covariates as the top model (FHD, 26.01 ha, $\beta = 0.54 \pm 0.19$, $p < 0.01$; PAVD_5_10, 15.21 ha, $\beta = 0.34 \pm 0.13$, $p < 0.01$) but also canopy cover (COVER, 15.21 ha, $\beta = -0.17 \pm 0.19$, $p = 0.39$). Models that included GEDI-fusion products outperformed those with only abiotic factors. Exemplifying this trend, a model that included only foliage height diversity as a univariate predictor ranked as the third best model (Appendix S1: Table S10). Most models without a GEDI-fusion covariate failed to outperform the NULL (Appendix S1: Table S10). The effect of study area followed the same trend where all study areas had variable but consistently positive coefficients. Tests of overdispersion indicated a good model fit for the whole model set with values between 0.81 and 0.86. For the top-ranking model, the conditional and marginal R^2 values were 0.73 and 0.43, respectively, indicating good total model fit and variance explained by fixed effects. Running the top-ranking model at the upper and lower 95% CIs of GLOR density estimates did not substantially alter results (Appendix S1: Figure S5).

The top-ranking NETO density model included elevation (Elev, 10.89 ha, $\beta = 0.48 \pm 0.11$, $p < 0.00$), plant area volume density above 20 m (PAVD_20, 136.89 ha, $\beta = -0.35 \pm 0.14$, $p = 0.01$), and foliage height diversity (FHD, 15.21 ha, $\beta = 0.27 \pm 0.09$, $p < 0.01$; Figure 4). There were no competitive models within $\Delta AIC_c < 2$. The study area had a significant effect ($p < 0.01$) where HJA was the reference, SIU positive, and UMP negative. The influence of the Site random effect was small

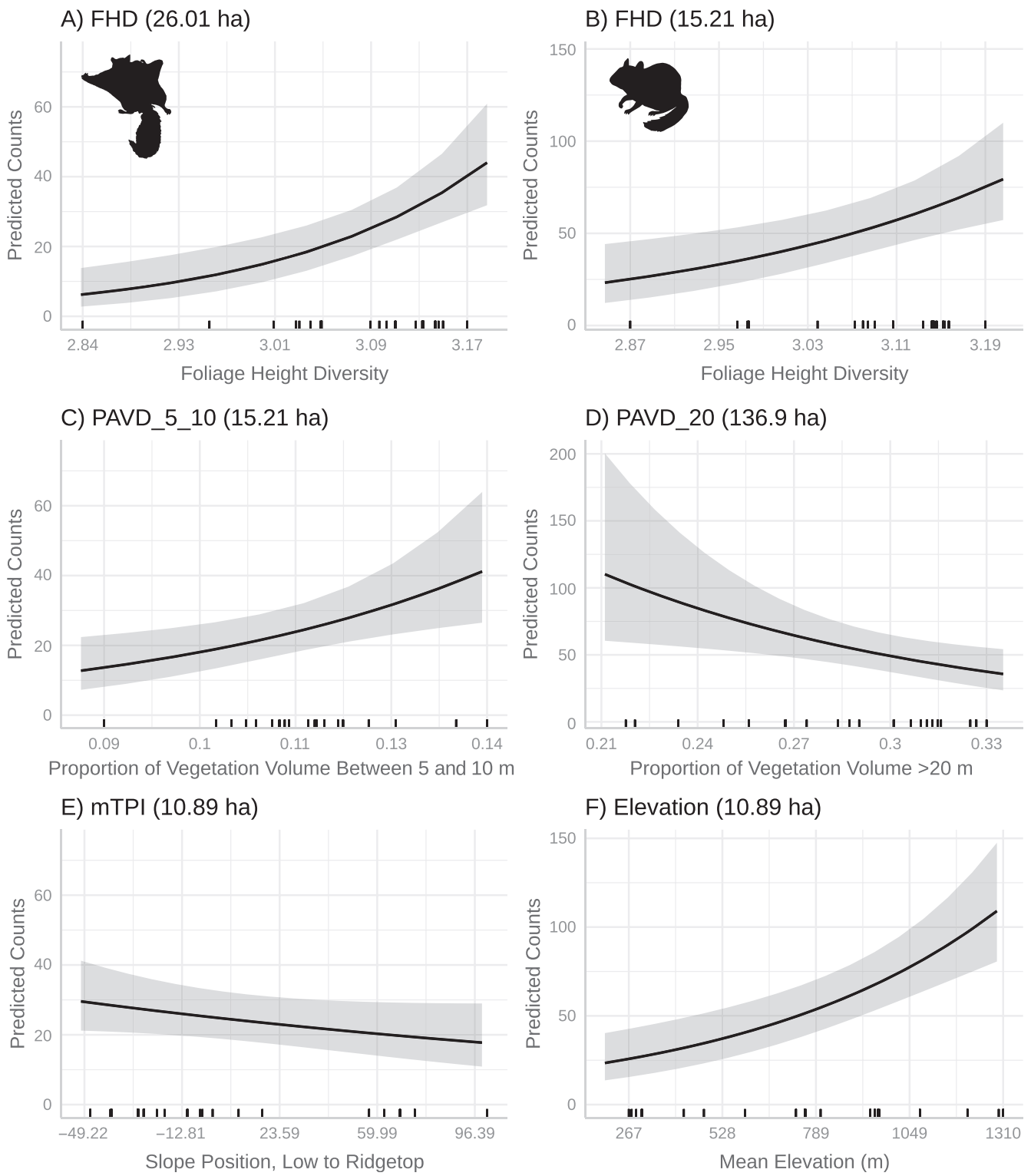

FIGURE 4 Marginal effect plots on density from the top models for *Neotamias townsendii* (right column) and *Glaucomys oregonensis* (left column). The title of each panel refers to the covariate and the optimized spatial scale used in each species' density model. The *x*-axis within each panel describes the variable and markings on the *x*-axis correspond to observed values at trapping grids. Covariate descriptions are as follows: Elevation, elevation; FHD, foliage height diversity; mTPI, topographic position index; PAVD_5_10, plant area volume density between 5 and 10 m; PAVD_20, plant area volume density above or below 20 m. See Table 1 for covariate descriptions. Image credits: *Glaucomys volans* and *Tamias striatus* images (sourced from PhyloPic) are by Chloé Schmidt and available under a CC BY 3.0 license, with no modifications made to the images for this work.

(var = 0.13, SD = 0.11), as was the influence of the YearStudy random effect, though the latter had a larger SD (var = 0.07, SD = 0.26) indicating greater temporal variation than was found for GLOR (Appendix S1: Figure S6). The conditional R^2 for this model was 0.61 and the marginal R^2 was 0.40. Overdispersion tests for the whole model set indicated a good fit with values between 0.73 and 0.87. This model was more sensitive than GLOR to upper and lower 95% density estimates (Appendix S1: Figure S6).

Using the top models for GLOR and NETO, we projected our density estimates to the area surrounding the H. J. Andrews Experimental and the Hebo District of the Siuslaw National Forest (Figure 5). Predicted densities (per hectare) of GLOR and NETO were generally higher surrounding the HJA than within the Hebo District (Figure 5).

DISCUSSION

The vertical and horizontal characteristics of vegetation are critical for managing and conserving wildlife species because these features are linked to much of the multidimensional space that comprises habitat

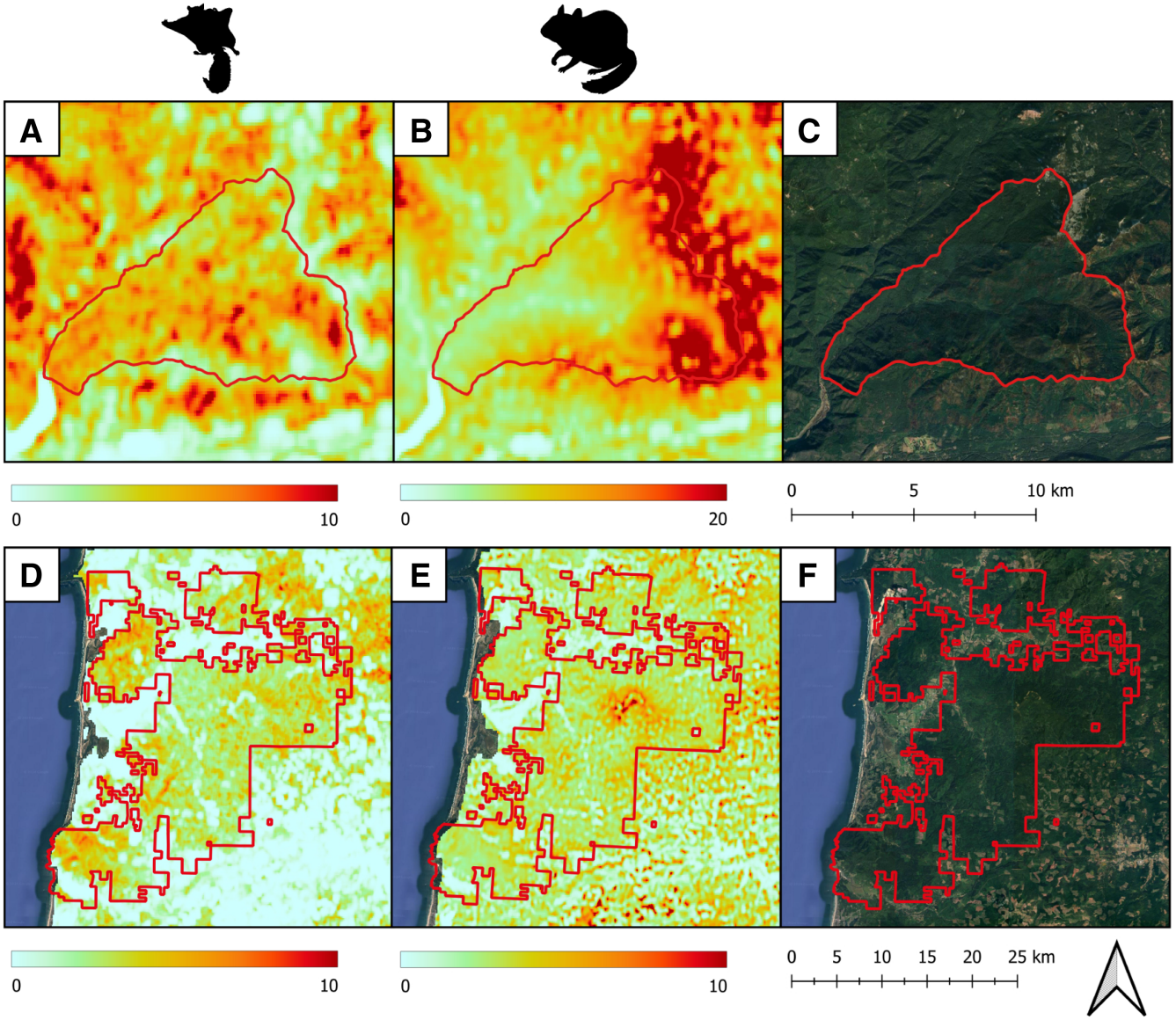

FIGURE 5 Projected density (in hectares) using the top model coefficients for *Glaucomys oregonensis* (left column) and *Neotamias townsendii* (right column). (A, B) are of the H. J. Andrews Experimental Forest. (D, E) are the Hebo District of the Siuslaw National Forest. (C, F) are reference images of each location from Google 2024. Image credits: *Glaucomys volans* and *Tamias striatus* images (sourced from PhyloPic) are by Chloé Schmidt and available under a CC BY 3.0 license, with no modifications made to the images for this work.

(Hall et al., 1997). Here, we present a novel approach to associate GEDI metrics, in the form of GEDI-fusion products, with wildlife demographic parameters. In doing so, we demonstrate the benefits of using demography to infer habitat quality, the importance of widely available datasets describing continuous forest structure for assessing these species' densities, and potential applications of GEDI for wildlife monitoring, conservation, and policy.

Robust demographic measures of habitat quality, such as survival and density, are rarely obtained directly because of logistical and financial constraints. A common alternative approach is to use species distributions generated from occurrence data with corresponding environmental data (McLoughlin et al., 2010), both of which are often easily obtained. These methods regularly form the backbone of conservation and management strategies despite the poor capacity to predict abundance, population mean fitness, and genetic diversity (Lee-Yaw et al., 2021). We leverage a new data set to test measures of habitat (i.e., GEDI-fusion products) by assessing whether they were predictive of key population parameters: density and survival. We found strong support that vertical aspects of the canopy were associated with the density of GLOR and NETO but in contrast to our hypotheses, weak support (i.e., competitive models $\Delta AIC_c < 2$) that survival related to GEDI-fusion products of forest structure for GLOR. Further, both species were present at all sites suggesting more coarse habitat indices leveraging occurrence data may have failed to identify the species–habitat relationships we did. Because survival was similar between sites, but density varied by orders of magnitude between sites, density appears to be a more useful metric in this instance for evaluating habitat quality. We acknowledge that caution should be taken while interpreting variation in density as differences in habitat quality (Robertson & Hutto, 2006; Van Horne, 1983), and that temporal cycling may obscure trends (Weldy, Epps, et al., 2019). Nevertheless, density is broadly representative of the carrying capacity of habitats because there must be adequate resources to support a population of a given size.

Our results confirm but also differ from aspects of our hypotheses while advancing the understanding of the ecology of these species. Both species displayed similar relationships to GEDI-fusion products of forest structure where density was strongly associated with these features, but survival was either weakly or not associated with forest structure, and the strength of these relationships did not vary by species as strongly as we hypothesized. The association of GLOR density to forest structure is consistent with Wilson (2010) who suggested that dense midstory and overstory vegetation mediates predation pressure to facilitate higher densities, however, we identified weak support that forest structure was directly related to survival itself. Less is known about the life history of NETO but they demonstrate flexible habitat preferences and characteristics of an r-selected species (Weldy et al., 2020). We contribute to this by identifying a strong elevational effect and suggest dense protective cover close to the ground (<20 m) and foliage height diversity are important. These findings differ from previous studies that found associations with coarse woody debris (Sultaire et al., 2021; Waldien, 2006) and canopy cover (Weldy, Epps, et al., 2019). For both species, our findings differ from previous studies by examining the influence of spatial scale beyond the trapping grid to demonstrate the influence of both relatively localized (10.89 ha) and relatively large (136.89 ha) effects of vegetation. Importantly, vegetation treatments are one of the few tools available to improve habitat conditions and our insights provide guidance on treatments to create conditions at certain localities (i.e., lower slopes and higher elevations) to improve habitat.

While we were able to identify statistically significant and meaningful relationships in our models, they represent oversimplifications of the processes that drive the spatiotemporal demographic patterns of these species. Notably, our density estimates were highly variable through time, especially for NETO, which suggests that more long-term studies like the H. J. Andrews Experimental Forest are needed to understand population dynamics. Specifically, additional primary occasions (trapping years) would likely have helped to improve the precision of density, survival, and other nuisance parameters (γ', γ'', p, and c) at Siuslaw and Umpqua sites (Schaub et al., 2004). Further, animal data that were specifically designed and collected to test the effects of remotely sensed forest structure on demography may yield stronger results rather than the studies we leveraged here. In addition, we may have failed to uncover a strong association between survival and GEDI-fusion products of forest structure because the survival of subclasses (e.g., male, female, young of year, etc.) vary more than the population as a whole, and survival has been shown to vary for GLOR based on age (Weldy et al., 2022). Alternatively, the resolution of the animal data (all individuals within a trapping grid) and environmental data (10.89 ha) may have been too coarse to understand these survival trends. Nevertheless, our analysis yielded reasonable performance given the complex nature of demography and the use of relatively few covariates.

The GEDI mission has generated considerable excitement by providing spatially extensive three-dimensional forest structure data. The use of full waveform, large footprint LiDAR systems such as GEDI is rare in wildlife studies (Acebes et al., 2021) and metrics obtained from

these systems are unfamiliar to most ecologists. We have demonstrated that full waveform metrics capture aspects of forest structure that wildlife responds to and should be more readily integrated into wildlife applications. GEDI-derived foliage height diversity has shown promise across a range of studies (Smith et al., 2022; Vogeler et al., 2023) including terrestrial or semi-arboreal mammals (this study, Smith et al., 2022). Indeed, foliage height diversity as a univariate predictor for GLOR density was the third best model. Several covariates that we anticipated being significant to GLOR density such as canopy cover and extent of old-growth forest were some of the best univariate predictors in the scale optimization process, but density models that included them were not highly supported. Their effects may have been washed out due to high collinearity with other predictors such as foliage height diversity, which may simultaneously capture aspects of both horizontal and vertical structure. Thus, while the use of these full-waveform LiDAR variables shows promise, there remains nuance in interpreting them for wildlife.

We have also shown that despite GEDI's relatively large footprint (25 m) and the subsequent resolution of the GEDI-fusion products (30 m), they can be effectively applied to animals that operate at small spatial scales. Others have demonstrated this for birds (Burns et al., 2020; Vogeler et al., 2023) but it also appears true for small-bodied mammals such as snowshoe hare (*Lepus americanus*; Smith et al., 2022), red squirrels (*Tamiasciurus hudsonicus*; Smith et al., 2022) and the species in this study. These findings suggest that future applications of GEDI data, or GEDI-fusion products can effectively be applied to a wide variety of taxa with varying body size and space use tendencies.

Explicit maps of forest structure, such as the GEDI-fusion products, have important implications for data-driven wildlife monitoring, conservation, and policy applications. Forest structure can be a controversial topic that cuts across scientific, social, and political arenas (e.g., the Northwest Forest Plan; Spies et al., 2019). Thus, accurate and widely available maps of structure can be used to ensure that discussions over long-term management plans are empirically grounded (Exec. Order No. 14072, 2022). We have shown that explicit maps of forest structure can be taken one step further by combining GEDI data with capture–mark–recapture data to create spatially explicit maps of realized wildlife density. Maps generated from density–habitat structure relationships can be used to predict how forest structure or changes in forest structure alter the density of species. Those insights can address the needs of managers who often manage their land in terms of stand structure to balance wildlife and socioeconomic needs (Kline et al., 2016). Further, realized density–habitat structure relationships can also be mapped across landscapes and through time (Davies & Asner, 2014; Eitel et al., 2016) to monitor changes in population size or incorporate density predictions into other studies (e.g., predator–prey relationships, species translocation efforts, etc.). We have demonstrated that it is possible to create such density maps, and this represents an important step to advance wildlife management while providing a direction for future research.

GEDI is a significant expansion in the availability of high-quality three-dimensional vegetation data but remains relatively underutilized for wildlife applications. Thus, our work is influential because we demonstrate that GEDI-derived data can effectively be used to predict animal density, a more meaningful habitat metric than previous uses of GEDI data in wildlife studies. The public availability of GEDI data, including the GEDI-fusion products, enables the framework presented here to be potentially replicated at the near global extent of GEDI coverage. Therefore, we suggest future applications of GEDI be used to assess how forest structure and changes in forest structure drive the density and assemblage of communities at spatial scales previously unattainable. Critical to these efforts will be the rich coverage of GEDI and continuous nature of the GEDI-fusion products developed from these reference data.

ACKNOWLEDGMENTS

We thank the many staff, technicians, and volunteers who collected the trapping data or helped to create the remote sensing products used. Without you, this work would not be possible. We also thank the USDA Forest Service Pacific Northwest Research Station, the Oregon State University Department of Fisheries, Wildlife and Conservation, and the Oregon State University Department of Forest Ecosystems and Society. The findings and conclusions in this publication are those of the authors and should not be construed to represent any official US Department of Agriculture or US government determination or policy. The use of trade or firm names in this publication is for reader information and does not imply endorsement by the US government of any product or service.

CONFLICT OF INTEREST STATEMENT

The authors declare no conflicts of interest.

DATA AVAILABILITY STATEMENT

Data and code (Barry, 2024) are available in Zenodo at https://doi.org/10.5281/zenodo.12765809.

ORCID

Brent R. Barry https://orcid.org/0000-0002-3077-4512
Joseph D. Holbrook https://orcid.org/0000-0002-7269-7690
Damon B. Lesmeister https://orcid.org/0000-0003-1102-0122

REFERENCES

Acebes, P., P. Lillo, and C. Jaime-González. 2021. "Disentangling LiDAR Contribution in Modelling Species–Habitat Structure Relationships in Terrestrial Ecosystems Worldwide. A Systematic Review and Future Directions." *Remote Sensing* 13: 3447.

Alston, J. M., M. J. Joyce, J. A. Merkle, and R. A. Moen. 2020. "Temperature Shapes Movement and Habitat Selection by a Heat-Sensitive Ungulate." *Landscape Ecology* 35: 1961–73.

Andruskiw, M., J. M. Fryxell, I. D. Thompson, and J. A. Baker. 2008. "Habitat-Mediated Variation in Predation Risk by the American Marten." *Ecology* 89: 2273–80.

Arbogast, B. S., K. I. Schumacher, N. J. Kerhoulas, A. L. Bidlack, J. A. Cook, and G. J. Kenagy. 2017. "Genetic Data Reveal a Cryptic Species of New World Flying Squirrel: *Glaucomys oregonensis*." *Journal of Mammalogy* 98: 1027–41.

Barry, B. R. 2024. "BrentBarry/GEDI_Squirrels_EcoApps2024: GEDI_Squirrels_EcoApps_2024 (v1.0.0)." Zenodo. https://doi.org/10.5281/zenodo.12765809.

Bates, D., M. Maechler, B. Bolker, and S. Walker. 2014. "lme4: Linear Mixed-Effects Models Using Eigen and S4." R Package Version 1, 1–23.

Bolker, B. M., M. E. Brooks, C. J. Clark, S. W. Geange, J. R. Poulsen, M. H. H. Stevens, and J. S. S. White. 2009. "Generalized Linear Mixed Models: A Practical Guide for Ecology and Evolution." *Trends in Ecology & Evolution* 24: 127–135.

Burnham, K. P., and D. R. Anderson. 2002. *Model Selection and Multimodel Inference: A Practical Information-Theoretic Approach*. New York: Springer Science & Business Media.

Burns, P., M. Clark, L. Salas, S. Hancock, D. Leland, P. Jantz, R. Dubayah, and S. J. Goetz. 2020. "Incorporating Canopy Structure from Simulated GEDI Lidar into Bird Species Distribution Models." *Environmental Research Letters* 15: 95002.

Cade, B. S. 2015. "Model Averaging and Muddled Multimodel Inferences." *Ecology* 96: 2370–82.

Carey, A. B., B. L. Biswell, and J. W. Witt. 1991. Methods for measuring populations of arboreal rodents. *USDA Forest Service General Technical Report*, Pacific Northwest Research Station, Portland, Oregon, USA.

Carey, A. B. 1995. "Sciurids in Pacific Northwest Managed and Old-Growth Forests." *Ecological Applications* 5: 648–661.

Carey, A. B., S. P. Horton, and B. L. Biswell. 1992. "Northern Spotted Owls: Influence of Prey Base and Landscape Character." *Ecological Monographs* 62: 223–250.

Cissel, J. H., F. J. Swanson, and P. J. Weisberg. 1999. "Landscape Management Using Historical Fire Regimes: Blue River, Oregon." *Ecological Applications* 9: 1217–31.

Cook, J. G., R. C. Cook, R. W. Davis, and L. L. Irwin. 2016. "Nutritional Ecology of Elk during Summer and Autumn in the Pacific Northwest." *Wildlife Monographs* 195: 1–81.

Cormack, R. M. 1964. "Estimates of Survival from the Sighting of Marked Animals." *Biometrika* 51: 429–438.

Davies, A. B., and G. P. Asner. 2014. "Advances in Animal Ecology from 3D-LiDAR Ecosystem Mapping." *Trends in Ecology & Evolution* 29: 681–691.

Dubayah, R., J. B. Blair, S. Goetz, L. Fatoyinbo, M. Hansen, S. Healey, M. Hofton, G. Hurtt, J. Kellner, and S. Luthcke. 2020. "The Global Ecosystem Dynamics Investigation: High-Resolution Laser Ranging of the Earth's Forests and Topography." *Science of Remote Sensing* 1: 100002.

Ecke, F., O. Löfgren, and D. Sörlin. 2002. "Population Dynamics of Small Mammals in Relation to Forest Age and Structural Habitat Factors in Northern Sweden." *Journal of Applied Ecology* 39: 781–792.

Eitel, J. U. H., B. Höfle, L. A. Vierling, A. Abellán, G. P. Asner, J. S. Deems, C. L. Glennie, P. C. Joerg, A. L. LeWinter, and T. S. Magney. 2016. "Beyond 3-D: The New Spectrum of Lidar Applications for Earth and Ecological Sciences." *Remote Sensing of Environment* 186: 372–392.

Elith, J., and J. R. Leathwick. 2009. "Species Distribution Models: Ecological Explanation and Prediction across Space and Time." *Annual Review of Ecology, Evolution, and Systematics* 40: 677–697.

Elliott, L. H., J. C. Vogeler, J. D. Holbrook, B. R. Barry, and K. T. Vierling. 2024. "Assessing GEDI Data Fusions to Map Woodpecker Distributions and Biodiversity Hotspots." *Environmental Research Letters: GEDI Special Issue* 19: 094027.

Farr, T. G., P. A. Rosen, E. Caro, R. Crippen, R. Duren, S. Hensley, M. Kobrick, M. Paller, E. Rodriguez, and L. Roth. 2007. "The Shuttle Radar Topography Mission." *Reviews of Geophysics* 45: RG2004.

Finke, D. L., and R. F. Denno. 2002. "Intraguild Predation Diminished in Complex-Structured Vegetation: Implications for Prey Suppression." *Ecology* 83: 643–652.

Forsman, E. D., R. G. Anthony, E. C. Meslow, and C. J. Zabel. 2004. "Diets and Foraging Behavior of Northern Spotted Owls in Oregon." *Journal of Raptor Research* 38(3): 214–230.

Fretwell, S. D., and H. L. J. Lucas. 1969. "On Territorial Behavior and Other Factors Influencing Habitat Distribution in Birds." *Acta Biotheoretica* 19: 16–36.

Froidevaux, J. S. P., F. Zellweger, K. Bollmann, G. Jones, and M. K. Obrist. 2016. "From Field Surveys to LiDAR: Shining a Light on How Bats Respond to Forest Structure." *Remote Sensing of Environment* 175: 242–250.

Fuller, A. K., D. J. Harrison, and H. J. Lachowski. 2004. "Stand Scale Effects of Partial Harvesting and Clearcutting on Small Mammals and Forest Structure." *Forest Ecology and Management* 191: 373–386.

Gaillard, J.-M., M. Hebblewhite, A. Loison, M. Fuller, R. Powell, M. Basille, and B. Van Moorter. 2010. "Habitat–Performance Relationships: Finding the Right Metric at a Given Spatial Scale." *Philosophical Transactions of the Royal Society B: Biological Sciences* 365: 2255–65.

Gillies, C. S., M. Hebblewhite, S. E. Nielsen, M. A. Krawchuk, C. L. Aldridge, J. L. Frair, D. J. Saher, C. E. Stevens, and C. L. Jerde. 2006. "Application of Random Effects to the Study of Resource Selection by Animals." *Journal of Animal Ecology* 75: 887–898.

Gorelick, N., M. Hancher, M. Dixon, S. Ilyushchenko, D. Thau, and R. Moore. 2017. "Google Earth Engine: Planetary-Scale Geospatial Analysis for Everyone." *Remote Sensing of Environment* 202: 18–27.

Gubert, L., F. Mathews, R. McDonald, R. J. Wilson, R. P. B. Foppen, P. Lemmers, M. La Haye, and J. Bennie. 2023. "Using High-Resolution LiDAR-Derived Canopy Structure and Topography to Characterise Hibernaculum Locations of the Hazel Dormouse." *Oecologia* 202: 1–13.

Guisan, A., S. B. Weiss, and A. D. Weiss. 1999. "GLM Versus CCA Spatial Modeling of Plant Species Distribution." *Plant Ecology* 143: 107–122.

Hall, L. S., P. R. Krausman, and M. L. Morrison. 1997. "The Habitat Concept and a Plea for Standard Terminology." *Wildlife Society Bulletin* 25(1): 173–182.

Hatten, J. R. 2014. "Mapping and Monitoring Mount Graham Red Squirrel Habitat with Lidar and Landsat Imagery." *Ecological Modelling* 289: 106–123.

Hayes, J. P., E. G. Horvath, and P. Hounihan. 1995. "Townsend's Chipmunk Populations in Douglas-Fir Plantations and Mature Forests in the Oregon Coast Range." *Canadian Journal of Zoology* 73: 67–73.

Holloway, G. L., and W. P. Smith. 2011. "A Meta-Analysis of Forest Age and Structure Effects on Northern Flying Squirrel Densities." *The Journal of Wildlife Management* 75: 668–674.

Huggins, R. 1989. "On the Statistical Analysis of Capture Experiments." *Biometrika* 76: 133–140.

Huggins, R. M. 1991. "Some Practical Aspects of a Conditional Likelihood Approach to Capture Experiments." *Biometrics* 47: 725–732.

Jaime-González, C., P. Acebes, A. Mateos, and E. T. Mezquida. 2017. "Bridging Gaps: On the Performance of Airborne LiDAR to Model Wood Mouse-Habitat Structure Relationships in Pine Forests." *PLoS One* 12: e0182451.

Johnson, C. J., K. L. Parker, and D. C. Heard. 2001. "Foraging across a Variable Landscape: Behavioral Decisions Made by Woodland Caribou at Multiple Spatial Scales." *Oecologia* 127: 590–602.

Johnson, D. H. 1980. "The Comparison of Usage and Availability Measurements for Evaluating Resource Preference." *Ecology* 61: 65–71.

Johnson, M. D. 2007. "Measuring Habitat Quality: A Review." *The Condor* 109: 489–504.

Jolly, G. M. 1965. "Explicit Estimates from Capture-Recapture Data with both Death and Immigration-Stochastic Model." *Biometrika* 52: 225–247.

Kendall, W. L., J. D. Nichols, and J. E. Hines. 1997. "Estimating Temporary Emigration Using Capture–Recapture Data with Pollock's Robust Design." *Ecology* 78: 563–578.

Kendall, W. L., K. H. Pollock, and C. Brownie. 1995. "A Likelihood-Based Approach to Capture-Recapture Estimation of Demographic Parameters under the Robust Design." *Biometrics* 51: 293–308.

Kennedy, R. E., Z. Yang, N. Gorelick, J. Braaten, L. Cavalcante, W. B. Cohen, and S. Healey. 2018. "Implementation of the LandTrendr Algorithm on Google Earth Engine." *Remote Sensing* 10: 691.

Kennedy, R. E., Z. Yang, and W. B. Cohen. 2010. "Detecting Trends in Forest Disturbance and Recovery Using Yearly Landsat Time Series: 1. LandTrendr — Temporal Segmentation Algorithms." *Remote Sensing of Environment* 114: 2897–2910.

Killion, A. K., A. Honda, E. Trout, and N. H. Carter. 2023. "Integrating Spaceborne Estimates of Structural Diversity of Habitat into Wildlife Occupancy Models." *Environmental Research Letters.* 18: 065002.

Kline, J. D., M. E. Harmon, T. A. Spies, A. T. Morzillo, R. J. Pabst, B. C. McComb, F. Schnekenburger, K. A. Olsen, B. Csuti, and J. C. Vogeler. 2016. "Evaluating Carbon Storage, Timber Harvest, and Habitat Possibilities for a Western Cascades (USA) Forest Landscape." *Ecological Applications* 26: 2044–59.

Knowles, J. E., and Frederick, C. 2019. merTools: *Tools for Analyzing Mixed Effect Regression Models. R package version 0.5.0*. https://cran.r-project.org/package=merTools

Kosterman, M. K., J. R. Squires, J. D. Holbrook, D. H. Pletscher, and M. Hebblewhite. 2018. "Forest Structure Provides the Income for Reproductive Success in a Southern Population of Canada Lynx." *Ecological Applications* 28: 1032–43.

Laake, J. L. 2013. "RMark: An R Interface for Analysis of Capture-Recapture Data with MARK." AFSC Processed Rep. 2013-01, Alaska Fish. Sci. Cent., NOAA, Natl. Mar. Fish. Serv., Seattle, WA. https://apps-afsc.fisheries.noaa.gov/Publications/ProcRpt/PR2013-01.pdf

Lee-Yaw, J. A., J. L. McCune, S. Pironon, and S. N. Sheth. 2021. "Species Distribution Models Rarely Predict the Biology of Real Populations." *Ecography* 6: e05877.

Linnell, M. A., R. J. Davis, D. B. Lesmeister, and J. K. Swingle. 2017. "Conservation and Relative Habitat Suitability for an Arboreal Mammal Associated with Old Forest." *Forest Ecology and Management* 402: 1–11.

MacArthur, R. H., and J. W. MacArthur. 1961. "On Bird Species Diversity." *Ecology* 42: 594–98.

McGarigal, K., H. Y. Wan, K. A. Zeller, B. C. Timm, and S. A. Cushman. 2016. "Multi-Scale Habitat Selection Modeling: A Review and Outlook." *Landscape Ecology* 31: 1161–75.

McLoughlin, P. D., D. W. Morris, D. Fortin, E. Vander Wal, and A. L. Contasti. 2010. "Considering Ecological Dynamics in Resource Selection Functions." *Journal of Animal Ecology* 79: 4–12.

Moriarty, K. M., C. W. Epps, and W. J. Zielinski. 2016. "Forest Thinning Changes Movement Patterns and Habitat Use by Pacific Marten." *The Journal of Wildlife Management* 80: 621–633.

Nakagawa, S., and H. Schielzeth. 2013. "A General and Simple Method for Obtaining R2 from Generalized Linear Mixed-Effects Models." *Methods in Ecology and Evolution* 4: 133–142.

Nelson, R., C. Keller, and M. Ratnaswamy. 2005. "Locating and Estimating the Extent of Delmarva Fox Squirrel Habitat Using an Airborne LiDAR Profiler." *Remote Sensing of Environment* 96: 292–301.

Pulliam, H. R. 2000. "On the Relationship between Niche and Distribution." *Ecology Letters* 3(349): 361.

R Core Team. 2023. *R: A Language and Environment for Statistical Computing*. Vienna: R Foundation for Statistical Computing. https://ww.R-project.org/.

Robertson, B. A., and R. L. Hutto. 2006. "A Framework for Understanding Ecological Traps and an Evaluation of Existing Evidence." *Ecology* 87: 1075–85.

Rosenberg, D. K., and R. G. Anthony. 1992. "Characteristics of Northern Flying Squirrel Populations in Young Second-and Old-Growth Forests in Western Oregon." *Canadian Journal of Zoology* 70: 161–66.

Rosenberg, D. K., and R. G. Anthony. 1993. "Differences in Townsend's Chipmunk Populations between Second-and Old-Growth Forests in Western Oregon." *The Journal of Wildlife Management* 57: 365–373.

Schaub, M., O. Gimenez, B. R. Schmidt, and R. Pradel. 2004. "Estimating Survival and Temporary Emigration in the Multistate Capture–Recapture Framework." *Ecology* 85: 2107–13.

Schooler, S. L., and H. S. J. Zald. 2019. "Lidar Prediction of Small Mammal Diversity in Wisconsin, USA." *Remote Sensing* 11: 2222.

Schulze, M., and G. W. Lienkaemper. 2015. "Vegetation Classification, Andrews Experimental Forest and Vicinity (1988, 1993, 1996, 1997, 2002, 2008) ver 7." Environmental Data Initiative. https://doi.org/10.6073/pasta/68296d816c9f4d8fe6e8bc3ed1668a5b.

Seber, G. A. F. 1965. "A Note on the Multiple-Recapture Census." *Biometrika* 52: 249–259.

Shirk, A. J., M. G. Raphael, and S. A. Cushman. 2014. "Spatiotemporal Variation in Resource Selection: Insights from the American Marten (*Martes americana*)." *Ecological Applications* 24: 1434–44.

Sikes, R. S., and Animal Care and Use Committee of the American Society of Mammalogists. 2016. "2016 Guidelines of the American Society of Mammalogists for the Use of Wild Mammals in Research and Education." *Journal of Mammalogy* 97: 663–688.

Smith, A. B., J. C. Vogeler, N. L. Bjornlie, J. R. Squires, N. C. Swayze, and J. D. Holbrook. 2022. "Spaceborne LiDAR and Animal-Environment Relationships: An Assessment for Forest Carnivores and Their Prey in the Greater Yellowstone Ecosystem." *Forest Ecology and Management* 520: 120343.

Spies, T. A., J. W. Long, S. Charnley, P. F. Hessburg, B. G. Marcot, G. H. Reeves, D. B. Lesmeister, M. J. Reilly, L. K. Cerveny, and P. A. Stine. 2019. "Twenty-Five Years of the Northwest Forest Plan: What Have We Learned?" *Frontiers in Ecology and the Environment* 17: 511–520.

Sullivan, T. P., D. S. Sullivan, and P. M. F. Lindgren. 2000. "Small Mammals and Stand Structure in Young Pine, Seed-Tree, and Old-Growth Forest, Southwest Canada." *Ecological Applications* 10: 1367–83.

Sultaire, S. M., A. J. Kroll, J. Verschuyl, and G. J. Roloff. 2021. "Stand-Scale Responses of Forest Floor Small Mammal Populations to Varying Size, Number, and Location of Retention Tree Patches." *Forest Ecology and Management* 482: 118837.

Turner, M. G., R. H. Gardner, R. V. O'neill, and R. V. O'Neill. 2001. *Landscape Ecology in Theory and Practice*, Vol. 401. New York: Springer.

Tweedy, P. J., K. M. Moriarty, J. D. Bailey, and C. W. Epps. 2019. "Using Fine Scale Resolution Vegetation Data from LiDAR and Ground-Based Sampling to Predict Pacific Marten Resting Habitat at Multiple Spatial Scales." *Forest Ecology and Management* 452: 117556.

Van Horne, B. 1983. "Density as a Misleading Indicator of Habitat Quality." *The Journal of Wildlife Management* 47: 893–901.

Vogeler, J. C., P. A. Fekety, L. Elliott, N. C. Swayze, S. K. Filippelli, B. Barry, J. D. Holbrook, and K. T. Vierling. 2023. "Evaluating GEDI Data Fusions for Continuous Characterizations of Forest Wildlife Habitat." *Frontiers in Remote Sensing* 4: 1196554.

Waldien, D. L., J. P. Hayes, and M. M. P. Huso. 2006. "Use of Downed Wood for Movement by Townsend's Chipmunks in Western Oregon." *Journal of Mammalogy* 87: 454–460.

Wasserman, T. N., S. A. Cushman, M. K. Schwartz, and D. O. Wallin. 2010. "Spatial Scaling and Multi-Model Inference in Landscape Genetics: *Martes americana* in Northern Idaho." *Landscape Ecology* 25: 1601–12.

Weldy, M., C. W. Epps, D. B. Lesmeister, T. Manning, and E. D. Forsman. 2020. "Spatiotemporal Dynamics in Vital Rates of Humboldt's Flying Squirrels and Townsend's Chipmunks in a Late-Successional Forest." *Journal of Mammalogy* 101: 187–198.

Weldy, M. J., C. W. Epps, D. B. Lesmeister, T. Manning, M. A. Linnell, and E. D. Forsman. 2019. "Abundance and Ecological Associations of Small Mammals." *The Journal of Wildlife Management* 83: 902–915.

Weldy, M. J., D. B. Lesmeister, and C. W. Epps. 2022. "Emigration Effects on Estimates of Age-and Sex-Specific Survival of Two Sciurids." *Ecology and Evolution* 12: e8833.

Weldy, M. J., T. M. Wilson, D. B. Lesmeister, and C. W. Epps. 2019. "Effects of Trapping Effort and Trap Placement on Estimating Abundance of Humboldt's Flying Squirrels." *PeerJ* 7: e7783.

Wilson, T. M. 2010. *Limiting Factors for Northern Flying Squirrels (Glaucomys sabrinus) in the Pacific Northwest: A Spatio-Temporal Analysis*. PhD Dissertation. Union Institute and University, Cincinnati, Ohio.

Wilson, T. M., and E. D. Forsman. 2013. *Density Management for the 21st Century: West Side Story*Gen. Tech. Rep. PNW-GTR-880. 79–90. Portland, OR: USDA.

Zuur, A. F., E. N. Ieno, N. J. Walker, A. A. Saveliev, and G. M. Smith. 2009. *Mixed Effects Models and Extensions in Ecology with R*, Vol. 574. New York: Springer Science Business Media.

SUPPORTING INFORMATION

Additional supporting information can be found online in the Supporting Information section at the end of this article.

How to cite this article: Barry, Brent R., Joseph D. Holbrook, Jody C. Vogeler, Lisa H. Elliott, Matthew J. Weldy, Damon B. Lesmeister, Clinton Epps, Todd Wilson, and Kerri T. Vierling. 2024. "Using Spaceborne LiDAR to Reveal Drivers of Animal Demography." *Ecological Applications* e3048. https://doi.org/10.1002/eap.3048